Enhanced resistance to organic fouling in a surface-modified reverse osmosis desalination membrane

Hafiz Zahid Shafi[a,b,*], Asif Matin[c], Zafarullah Khan[a]

[a]*Department of Mechanical Engineering, King Fahd University of Petroleum & Minerals (KFUPM), Dhahran 31261, Saudi Arabia, Tel. +966 568429622; email: hafizahid@kfupm.edu.sa (H.Z. Shafi), Tel. +966 13 860 2693; email: zukhan@kfupm.edu.sa (Z. Khan)*
[b]*Center of Excellence in Desalination, RI, KFUPM, Dhahran 31261, Saudi Arabia*
[c]*Center for Engineering Research, KFUPM, Dhahran 31261, Saudi Arabia, Tel. +966 13 8601856; email: amatin@kfupm.edu.sa*

ABSTRACT

Membrane surface modification with the aim of lowering foulant to surface affinity, has recently gained considerable attention. In this article, we report improved performance (permeate flux, salt rejection, and resistance to alginate fouling) of surface-modified reverse osmosis (RO) membranes, under cross-flow filtration conditions. The surface of RO membranes was modified by amphiphilic hydroxethyl methacrylate-co-perfluorodecyl acrylate (HEMA-co-PFDA) copolymer films. The amphiphilic coatings were deposited via an all-dry and solventless vapor deposition technique, termed as initiated chemical vapor deposition. Scanning electron microscopy revealed that a dense and continuous layer of alginate formed on the surface of the unmodified membranes, whereas foulant deposition on the surface-modified membranes was found to be more sporadic and discontinuous. The coatings were found stable even after 6 h of exposure to sodium alginate at higher pressure (800 psi), as evidenced by ATR-FTIR analysis of the post-fouled membranes.

Keywords: Surface modification; Amphiphilic copolymer coatings; Cross-flow filtration; Organic fouling

1. Introduction

Reverse osmosis (RO) process is gaining rapid market share in seawater/brackish water desalination, drinking, and wastewater treatment industry. Predominantly, the interest is the use of RO membranes in seawater and advanced wastewater reclamation to increase limited available clean water supply. RO technology which is a rather simple and environment-friendly process faces a serious economic drawback due to the fouling of membranes, and the RO membranes can be considered as the heart of the RO process. Membrane fouling is an inevitable phenomenon in almost all the membrane-based filtration/separation processes, and can be categorized into several classes, but biofouling and organic fouling being the most severe ones [1–5]. The former is caused by the adhesion and/or irreversible attachment of micro-organism onto the surface of RO membrane and subsequent biofilm formation; and is considered a serious concern in membrane-based water desalination industry, whereas the latter being a major concern for secondary effluent

*Corresponding author.

plants. Considerable amount of organic substances present in waste water (termed as effluent organic matter) results in the formation of organic fouling, limiting an efficient application of RO membranes [6,7].

In biofouling, initially, the intermolecular adhesion between the bulk foulant and the foulant deposited on the membrane surface controls the evolution of fouling layer [8]. Firstly, in most practical applications, foulant–foulant interactions govern the kinetics of fouling layer formation, and secondly, these interactions also dictate the structure (compactness and thickness) of fouling layer. The second effect determines hydraulic resistance of the deposited fouling layer and, hence, flux decline during fouling [9].

Fouling of microfiltration and ultrafiltration membranes by biopolymer adsorption (such as proteins) has been extensively studied, however, very little is known on organic fouling of RO membranes [9,10]. Organic fouling may be caused by the biomolecule foulant present in the feed water. These biomolecule foulants are represented by three important classes, namely proteins, polysaccharides, and natural organic matter (NOM). Proteins and alginate adsorption on an RO membrane surface is known to play a direct role in membrane biofouling, with protein providing the food for bacteria and alginate being the major part of the extracellular polymeric substances [11,12] in the biofilm matrix.

Earlier, we have reported the synthesis of amphiphilic hydroxethyl methacrylate-co-perfluorodecyl acrylate (HEMA-co-PFDA) copolymer coatings [13] using *initiated* chemical vapor deposition (*i*CVD) technique, which allowed solventless deposition under near ambient conditions without damaging delicate substrate such as RO membranes. Furthermore, these coatings were found to show anti-biofouling behavior under static conditions [12]. In this article, we focused on evaluating the fouling resistance of the surface-modified RO membranes (with HEMA-co-40% PFDA copolymer films) against deposition of biopolymers that are believed to play a catalytical role in promoting the attachment of bacteria, and ultimate formation of biofilm. This was accomplished by comparing the performance (permeate flux, salt rejection, and resistance to organic fouling) of modified and bare Koch membranes (TFC-HR) under cross-flow permeation tests in a model organic foulant–sodium alginate (SA). Surface morphology and compositional analyses of the fouling layer deposited on the modified and bare RO membranes surfaces were investigated by scanning electron microscopy (SEM) and ATR-FTIR, respectively.

2. Experimental

2.1. Materials

All the chemicals for thin-film synthesis including monomers hydroxethyl methacrylate (HEMA), perfluorodecyl acrylate (PFDA), and initiator *tert*-butyl peroxide (TBPO) were purchased from Sigma Aldrich, USA, and were used without further purification. The feed water for cross-flow permeation tests was prepared from analytical grade sodium chloride (NaCl) completely dissolved in deionized (DI) water (with resistivity 18.2 M Ω cm, from Barnstead™ NanoPour™, Thermo Scientific). The foulant SA was purchased from Sigma Aldrich, USA; specified dosages of SA were introduced into the feed water. RO membranes (TFC-HR, from Koch membranes systems), hereafter, referred to as Koch membranes were used for this study.

2.2. Synthesis of HEMA-PFDA copolymer coatings

HEMA-PFDA copolymer coatings were deposited on commercial Koch membranes in custom built *i*CVD reactor, (Sharon Vacuum) by allowing the controlled flow of the two monomers and letting them to react with the initiator TBPO on heated filament, while the copolymer was deposited on the substrate (Koch membranes) placed on the cooled stage. Details of the *i*CVD reactor [14,15] and synthesis of amphiphilic HEMA-PFDA copolymer coatings have been describe earlier [12,13].

2.3. Cross-flow permeation tests

Performance evaluation (permeate flux, % salt rejection, and resistance against alginate fouling) of duplicate unmodified and modified Koch membrane specimens were conducted on a test rig based on a cross-flow permeation cell (CF 042, from Strelitech™ Corp., USA). For this purpose, 6×10 cm^2 samples of modified and unmodified Koch membranes were placed in the cell and DI water at a pressure of 800 psi at 27°C (±2°C) was passed in a cross-flow manner. The feed water was unbuffered with a constant pH value of around 6.0 (±0.5). Details of the permeation test setup, has already been described in our earlier study [16].

Membranes were compacted for at least 18–20 h before taking permeate flux measurements. Permeate was collected in a measuring cylinder for five minutes. Three readings were taken for each specimen every half hour in this way, converted to L/m^2 h, and the average value reported as the permeate flux of the membrane under test. Sodium chloride was first dissolved thoroughly in a beaker and then added to

the feed tank to make the final concentration of 2,000 mg/L. After half hour of stabilization with the saltwater, three readings of permeate flux were recorded every half hour up to 1 h and average value of the three readings reported as permeate flux (after salt addition). The concentration of salt in the permeate was measured using a conductivity meter (YSI-3200, Conductivity instruments, Yellow Spring, OH, USA) equipped with a type 3252 conductivity cell. Finally, the percentage salt rejection (%R) was calculated using the following relation:

$$\%R = (CF - CP)/CF$$

where CF and CP are the concentrations of salt in feed and permeate, respectively.

Following the salt addition, SA was first thoroughly dissolved in small volume of DI water by magnetic stirring and then added to feed water to make feed water concentration of 100 mg/L. After the introduction of SA into the feed, 1 h was given for stabilization, and permeate flux was recorded after every hour for the next 6 h. Two readings were taken every hour for each specimen in this way.

2.4. Scanning electron microscopy

Post-fouling surface topology of the membrane samples was examined by SEM (JEOL, JSM, 6460LV, Japan). Small portions (~0.5 cm^2 area) of triplicate fouled membrane (both modified and bare Koch) samples were cut and fixed on to specimen stage with double-sided copper tape, sputter coated for 5 min, and were then observed under SEM.

2.5. Compositional analysis

For compositional analyses of the clean and fouled membrane surfaces, ATR-FTIR (Nicolet 8700 FTIR) spectrometer coupled to a germanium crystal was used. OMNIC 6.2 software (Thermo Electron Corp., Hampton, NH) was employed to obtain the ATR-FTIR spectra. At least two replicate samples were analyzed from each membrane. Five scans were taken from different points of each sample. Each spectrum represents an average of 16 scans collected in the range 600 – 4,000 cm^{-1} at a resolution of 1 cm^{-1}.

3. Results and discussion

3.1. Cross-flow permeation tests

Presented in Fig. 1 are the permeate flux (before and after salt addition) and salt rejection performances of the modified (with 30 nm (±3 nm) thick HEMA-co-40% PFDA copolymer film) and bare (unmodified) Koch membranes. Average permeate flux of bare Koch membranes was found to be 126.3 (±4.5) L/m^2 h, whereas Koch membranes coated with HEMA-co-40% PFDA copolymer films yielded average permeate flux of 116.5 (±3.0) L/m^2 h. The slightly lower permeate flux of modified RO membranes are due to the additional copolymer film over the active polyamide layer and are consistent with our previous studies [3,17,18]. The two gray bars on the right in Fig. 1 symbolize virtually the same percentage salt rejection (98.9% (±0.3%) and 99.1% (±0.2%), respectively, for bare and modified Koch membranes). The error bars show one standard deviation from the mean of six measurements taken every half hour for flux computation. At first glance, these results may appear comparable with regard to permeation and separation (salt rejection) performances of bare and modified Koch membranes. However, during the first hour of salt addition, permeate flux declines more rapidly (from 122.6 to 116.4 L/m^2 h) for the case of unmodified Koch membranes compared to virtually no decline (from 116.5 to 115.4 L/m^2 h) for modified Koch membranes as shown in Fig. 2 indicating better permeation and similar salt rejection performances of the modified membranes in the presence of salt.

The overall salt rejection of both the membranes (bare and the modified) is measured to be around 99% and the chemical composition of the coatings has no effect on the salt rejection. The salt rejection percentages for bare and coated membranes at the end of 7 h are observed to be constant throughout the
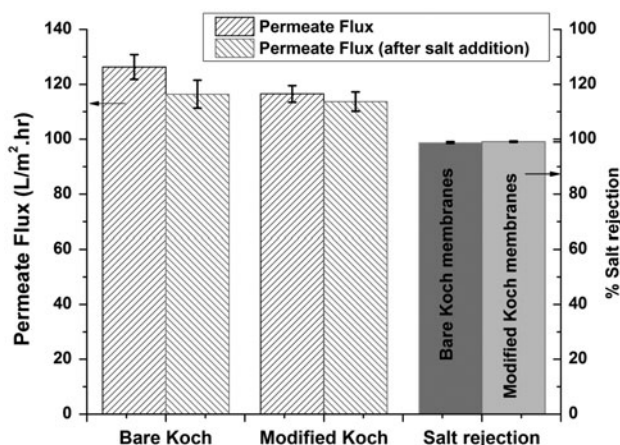

Fig. 1. Permeate flux and salt rejection of unmodified (bare) and modified (with ~35 nm thick HEMA-co-40% PFDA copolymer film) Koch membranes under cross-flow filtration conditions at 800 psi and 27°C (±2°C).
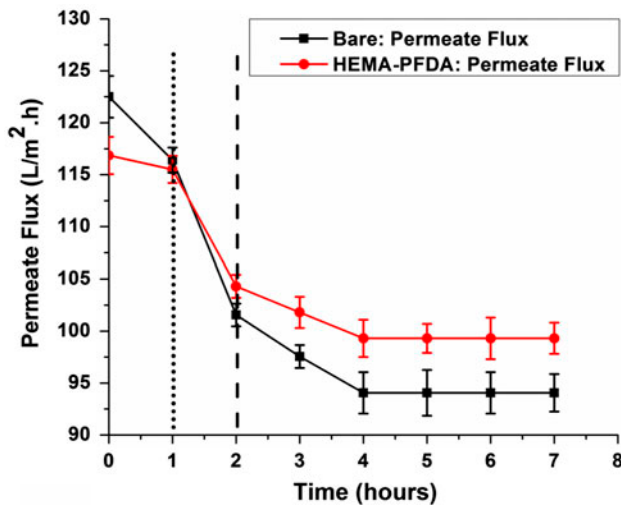
Fig. 2. Permeate Flux as a function of time in the presence of SA (100 mg/L) and salt (2,000 mg/L). Upper curve (red) and lower curve (black) represent, respectively, for modified and bare Koch membranes. Dotted and dashed lines represent the time after 1 h of salt (NaCl) and SA addition, respectively.

experiments. This can be explained by the fact that the thickness of the deposited amphiphilic copolymer (30 nm) film is only 12% of the thickness of polyamide active layer (assuming its thickness to be 250 nm). Although the copolymer film does swell upon exposure to water, but for amphiphilic chemistry (~40% PFDA), the rate of water uptake is very slow and the swelling is negligible [19]. Therefore, the hydrated thickness can be assumed to be nearly the same as the thickness without water exposure.

The salt rejection performances of the modified Koch membranes are compared with other thin-film composite membranes. Ghosh et al. [20] reported the salt rejection of the standard polyamide thin-film composite (TFC) RO membranes (prepared by interfacial polymerization from m-phenylenediamine trimesoyl chloride layer on polysulfone supports) to be varied between 83 and 94% at 2,000 ppm of NaCl solution. Similar salt rejection value of 79–95% was reported for polyamide (TFC) membranes on plasma-treated polysulfone substrates [21]. In another study performed on plasma-treated polysulfone substrates, with interfacially polymerized polyamide active layer, salt rejection of 94–98% at 2,000 ppm of NaCl solution was reported [22]. Together with the rejection results, the presence of these coatings does not seem to adversely affect the membrane performance in a significant manner. We have recently reported the enhanced resistance to organic fouling of RO membrane surface-modified with the HEMA-co-40% PFDA copolymer

coatings under higher salt loadings (salt concentration closer to seawater: 20,000 mg/L) [23]. The current findings in conjunction with our recently published report prove that the deposited amphiphilic coatings are alginate fouling resistant under both brackish as well as seawater conditions.

Likewise, contrasting results were found when the two membranes were exposed to a solution of organic foulant (SA), a model polysaccharide (present in seawater). During the first hour of SA addition, faster initial flux decline (from 116.4 to 100.3 L/m^2 h) was observed for the case of bare Koch membranes that corresponds to ~15% flux decline. As opposed to bare Koch membranes, permeate flux of modified Koch membranes during the first hour of SA addition decreased from 115.4 to 105.0 L/m^2 h that corresponds ~9% flux decline. As a result, modified Koch membranes depict ~60% less flux decline as compared to the counterpart bare membranes during first hour of exposure to SA at 800 psi. Error bars shown in Fig. 2 represent standard deviation from the mean flux calculated from the four measurements taken at a given time interval.

Greater slope/rate of flux decline observed for the bare Koch membranes (black line in Fig. 2) during first hour of exposure to SA is a clear indication of larger drag force between the membrane surface and the foulant (SA). This higher drag force is presumably due to the stronger membrane–foulant interaction (adhesion) and encourages the continuous deposition of fouling layer onto the surface of membrane (Fig. 5(c) and (d)). On the same basis, lower flux decline observed during the first hour of SA exposure for the case of modified membranes, is an evidence of disrupted foulant adhesion onto the surface of modified membranes and is attributed to the presence of amphiphilic copolymer (HEMA-co-40% PFDA) coating that obstructs the formation of foulant (Fig. 5(a) and (b)).

Similarly, during the next 2 h of alginate exposure, moderate flux decline ~7 and ~4% was observed, respectively, for bare and modified Koch membranes. As a result, modified membranes show ~57% less permeate flux decline when compared to unmodified Koch membranes for the same duration. The permeate flux of both bare and modified Koch membranes, finally, levels off after 4 h of SA addition. Similar results were found by Widjaya et al. [24] who have shown that major fouling by alginate occurs during the initial few hours (first four hours) of exposure to SA.

It is well documented that surface hydrophilicity is a major determinant of membrane fouling tendency [25]. Hydrophilic surfaces attract a strongly bound water layer which acts as a buffer, minimizing direct

foulant–surface interaction and discouraging hydrophobic–hydrophobic interactions [13]. Given the fact that the foulants that are found in different water environments (brackish water, seawater etc.) are diverse (hydrophobic and hydrophilic) in nature, a hydrophilic surface might not be the ideal one. For example, membrane surface hydrophilicity has a negative effect on membrane fouling by NOM, for which the hydrophilic components have been identified as major foulants [26]. With the above in mind, an efficient antifouling surface would be an appropriate mix of hydrophilic and hydrophobic constituents at microscopic level. Molecular-scale compositional heterogeneity of the HEMA-PFDA copolymer films has already been reported to confuse/discourage the adhesion/attachment of protein (BSA) molecules [19]. In the case of BSA (predominantly hydrophobic), the pure HEMA surface is more resistant to adsorption than the pure PFDA monomer. However, in the case of SA (predominantly hydrophilic), the situation is reversed with the hydrophilic HEMA showing enhanced adsorption [27].

It is worth mentioning that much lower permeate flux decline (observed only for the modified Koch membranes) particularly during the first three hours of alginate exposure is attributed to the amphiphilic copolymer (HEMA-co-40% PFDA) coatings. This can be elucidated by the existence of functional groups on the membrane surfaces that have been found to influence the adsorption of alginate [28] and other organic foulants [29]. It is important to mention that membrane surface rich in –OH functional group has been reported to resist alginate fouling [30,31]. The

deposited amphiphilic copolymer coatings (with –OH surface moieties) are believed to discourage/hinder the membrane–foulant (SA) interaction in a much similar way as their reduced interaction with bacteria [13,24] and protein [19] reported earlier. Schematic antifouling mechanism of RO membrane surface-modified with the amphiphilic copolymer coatings is elucidated in Fig. 3. The basis of the reduced membrane–foulant interaction is further explained in Section 3.2.

3.2. SEM analysis

Reduced water flux and compromised permeate quality are the two main adverse effects of membrane fouling. Therefore, it is of paramount importance to understand the mechanisms which govern organic fouling for sustainable application of RO membranes technology [32].

Foulant deposition on the membrane surface depends on foulant–membrane surface interaction and determines the structure, thickness, and compactness of the deposited foulant layer. Foulant–foulant interactions are also held responsible for the fouling layer structure formation, which determines the hydraulic resistance of the fouling layer and, in turn, the flux decline behavior during fouling [9].

Optical examination of the fouled membrane surfaces shows a very thin light yellow color layer of the foulant (SA) deposited on the modified membranes as opposed to a dark brown and dense foulant layer on the bare Koch membranes (Fig. 4). The digital camera photo indicates that the foulant layer on the modified
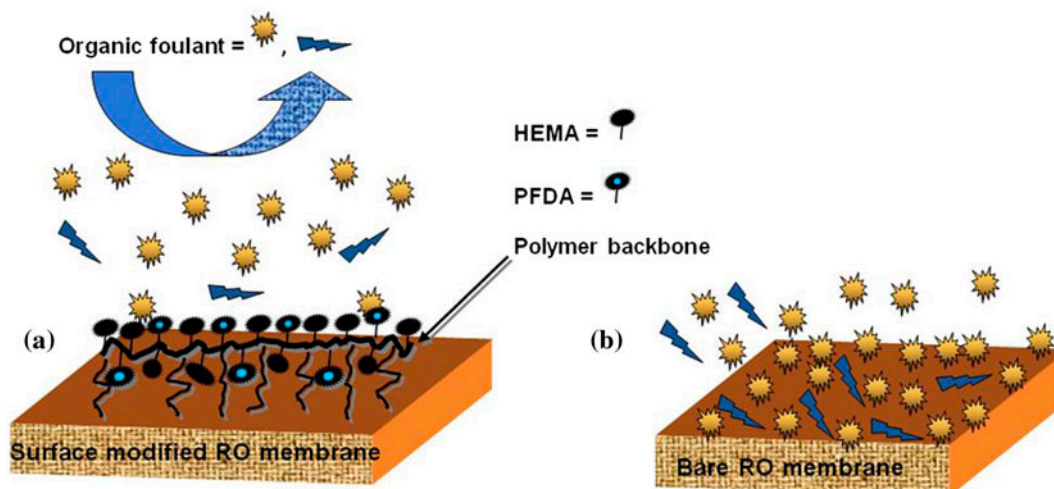

Fig. 3. Schematics showing the antifouling mechanism of RO membranes surface-modified with HEMA-co-40% PFDA films (a) deposited on commercial RO membranes. Bare RO membrane (b) is presented for the sake of comparison.
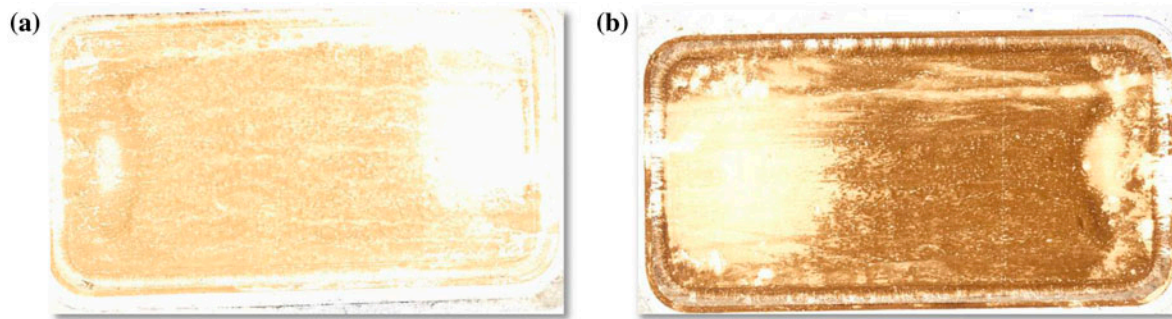
Fig. 4. Digital camera images of (a) modified and (b) unmodified Koch membrane samples after 6 h of exposure to model organic foulant (sodium alginate) under the cross-flow filtration conditions at 800 psi. The light yellow color of the sporadically deposited alginate layer is clear on the modified Koch membrane, whereas dark brown, dense, and continuous alginate layer is obvious on unmodified Koch membrane.

membranes is discontinuous and patchy in structure. More detailed surface morphology of the deposited alginate layer was investigated by SEM. Fig. 5 shows the representative SEM images of the post-fouled modified and unmodified Koch membranes taken at two different magnifications (2,000 and 7,000×). It is worth noting that the foulant deposition on the modified membrane surface is quite sporadic and porous in
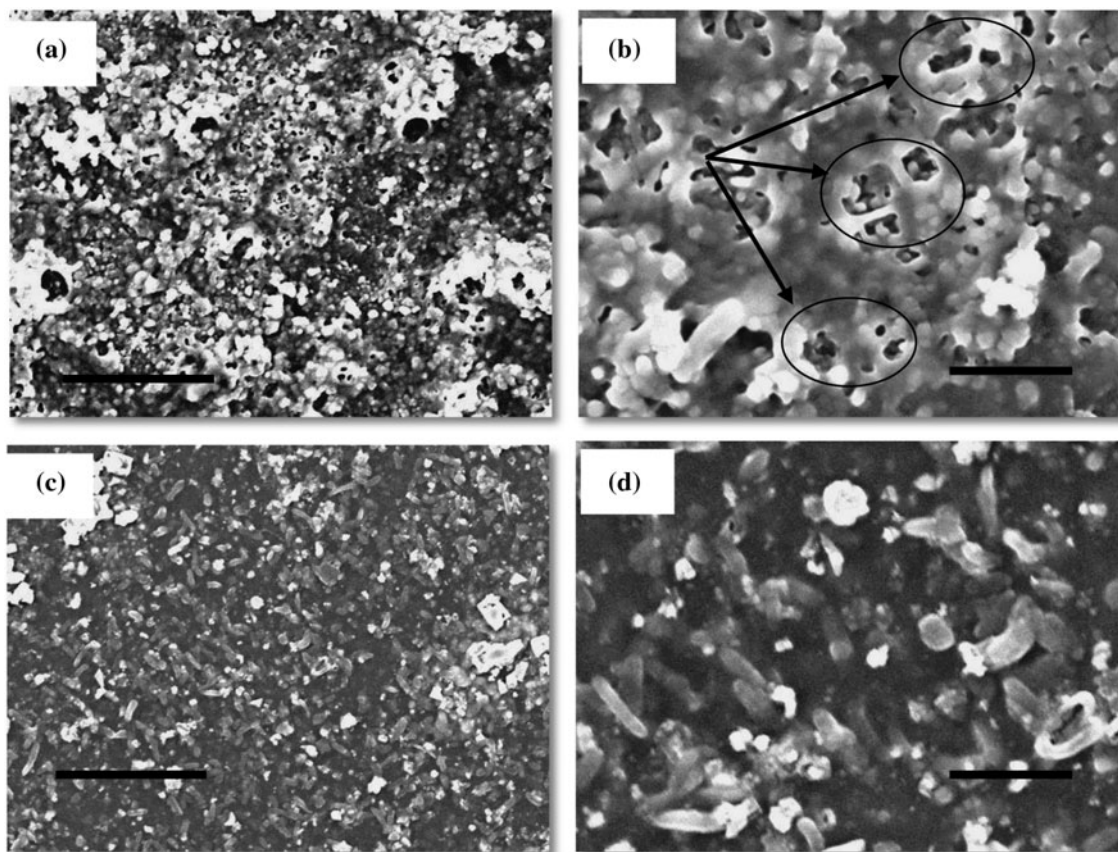

Fig. 5. Surface morphology of: (a, b) coated (modified) and fouled Koch membranes and (c, d) uncoated (unmodified) and fouled Koch membranes after 6 h of exposure to SA solution (100 mg/L in DI water) at pressure of 800 psi. Fig. (a, c) taken at 2,000× with scale bar 10 μm, whereas Fig. (b and d) taken at 7,000× with scale bar 2 μm. Highlighted in ovals are the pores in foulant layer.
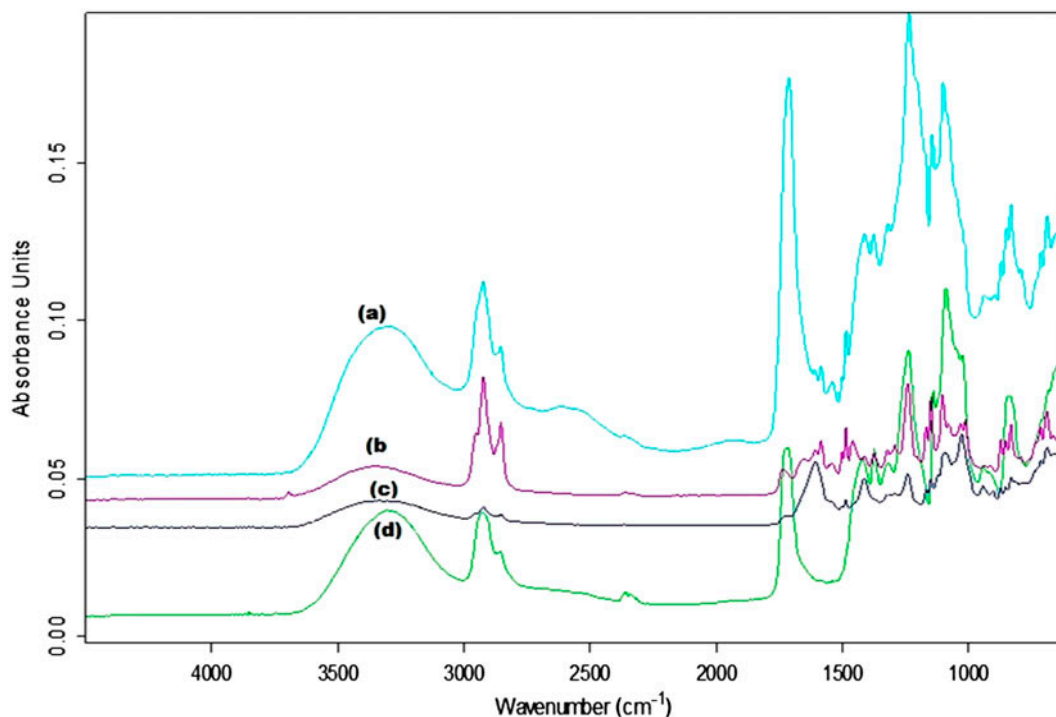
Fig. 6. ATR-FTIR spectra of Koch membranes: (a) coated and clean, (b) coated and fouled, (c) uncoated and fouled, and (d) uncoated (bare) and clean. Dashed and dotted black lines show stretching of –CH and carbonyl groups at ~2,950 and ~1,730 cm^{-1}, respectively.

its morphology as opposed to a dense and continuous foulant deposition on unmodified (bare) Koch membrane surface. This sporadic, discontinuous, and porous deposition of foulant is attributed to the thin-surface coating of HEMA-co-PFDA copolymer on the modified membranes that discourages the attachment of alginate on membrane surface. This hindered/reduced attachment of foulant (SA) on the membrane thus results in a much lower flux decline with time in the modified Koch membranes (when compared to the unmodified Koch membranes) as discussed earlier in Section 3.1.

3.3. ATR-FTIR analysis

In order to investigate any chemical change that could be associated with the exposure of membranes to SA, ATR-FTIR spectra of both the modified and unmodified Koch membranes before and after SA fouling were compared. For this purpose, FTIR spectra were obtained in the range of 600–4,000 cm^{-1}. Fig. 6 illustrates the complete spectra for Koch membranes in both states, i.e. coated (a) and uncoated (d), whereas spectra (b) and (c) in Fig. 6, respectively, represent the modified and unmodified Koch membranes after fouling by SA. For wave numbers less than

2,500 cm^{-1}, the penetration depth is more than 300 nm probing both the polyamide layer and the polysulfone support layer present in RO membranes. In contrast, the higher wave number regions (~2,700–3,700 cm^{-1}) focus on the chemical characteristics of the top layer (<200 nm) [33].

It can be seen that all the three spectra are quite similar, though not identical in all respects. Almost all the characteristic peaks revealing the presence of the polyamide and polysulfone layers are present in the spectra of both samples in their clean states. Peaks around 1,541, 1,609, and 1,663 cm^{-1} are assigned to amide two bands, aromatic amide, and amide one band, respectively [34]. More noticeable difference between the modified and unmodified Koch membranes before exposure to SA is the presence of strong peak at ~1,730 cm^{-1} in the modified membranes (sky blue and green curve in Fig. 6). This peak is ascribed to the carbonyl stretching present in the HEMA-PFDA units. Similarly, peaks at ~3,300 and ~2,950 cm^{-1} are observed in both uncoated and the surface-modified Koch membranes before exposure to SA. The former broader peak has been reported as a complex peak that comprises N–H and O–H stretching, whereas the latter peak corresponds to the aliphatic C–H stretching, and both peaks arise from the polyamide layer of TFC-RO
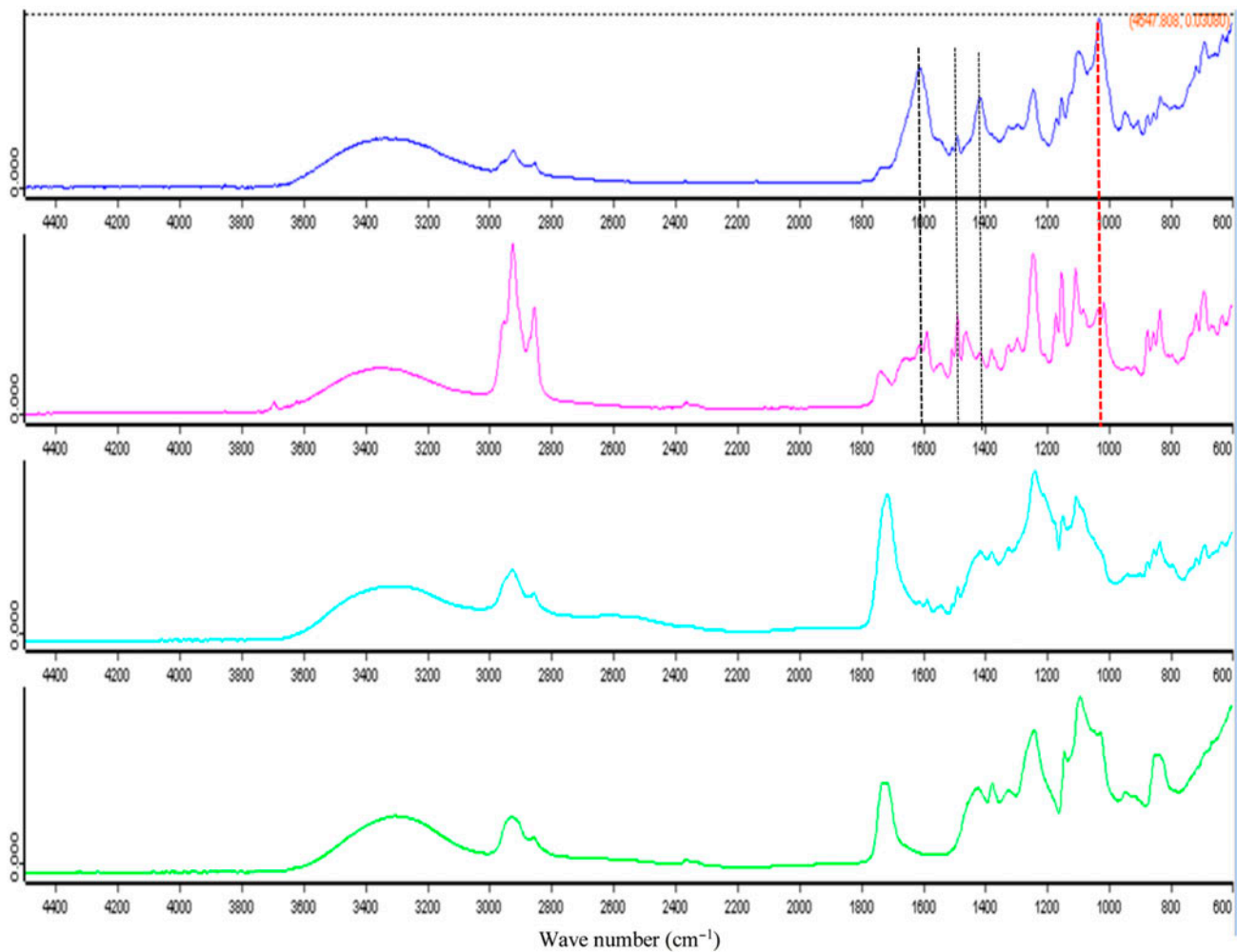
Fig. 7. FTIR spectra of Koch membranes before and after fouling with SA. Black lines show peaks associated to the symmetric and asymmetric stretching of carboxylate (–COO) groups and red line indicates bending of –OH groups present in alginate.

membranes [33]. However, it is important to note that, compared with the spectrum of neat uncoated Koch membranes (Fig. 6(d)), the intensity of peak at ~3,300 cm^{-1} is larger for the case of surface-modified Koch membranes and is attributed to the presence of –OH surface moieties in the modified RO membranes (Fig. 6(a)). It is worth noticing that for the coated membrane (sky blue curve), the main peak at 2,950 cm^{-1} is sharper (black dashed line), and also the nearby smaller peak is more well defined than for the virgin polyamide (green curve). This apparent difference between the shapes of the two peaks can be explained by the presence of extra C–H groups on the HEMA-co-PFDA copolymer of the modified membrane.

After the deposition of alginate, both the characteristic peaks at ~3,300 and ~2,950 cm^{-1} in the higher wave number regions (3,700–2,700 cm^{-1}) are diminished but still visible at approximately the same location. This could be the result of the copolymer (HEMA-co-PFDA) film and the PA layer of the membrane being masked by the foulant layer on top. However, again the noticeable difference is that the intensity of the peak at ~2,950 cm^{-1} is diminished substantially in the spectrum of uncoated membranes (Fig. 7(a)) compared to the spectrum of the modified membranes (Fig. 7(b)) after alginate fouling. As pointed out earlier, this significant difference can be explained by the presence of extra C–H groups on the HEMA-co-PFDA copolymer of the modified membrane.

In fact, the trend of peak diminishing is also seen for most of the peaks with wave number below 1,700 cm^{-1}. In general, the spectrum of the fouled and coated membrane in Fig. 7(b) (pink curve) has more
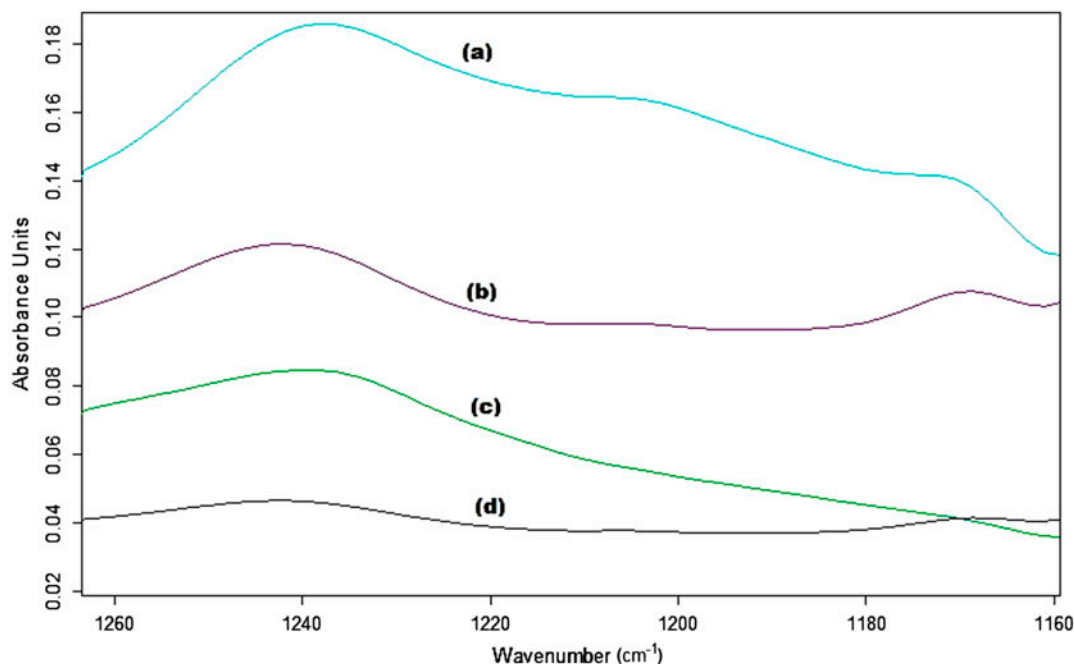
Fig. 8. ATR-FTIR spectra of Koch membranes: (a) coated and clean, (b) coated and fouled, (c) uncoated and clean, and (d) uncoated and fouled.

resemblance to that of the neat and coated membrane in Fig. 7(c) (sky blue curve). However, in both the virgin and the modified Koch membranes after fouling with SA, the emergence of new peaks at ~1,610, ~1,500, 1,410, and ~1,030 cm^{-1} was observed (highlighted by dashed lines in Fig. 6 for the two fouled membranes only). The first peak corresponds to symmetric (~1,610 cm^{-1}) stretching, whereas the peaks at ~1,500, 1,410 cm^{-1} are assigned to asymmetric stretching of carboxylate, and the peak at 1,035 cm^{-1} is ascribed to –OH bending groups present in the alginate layer (red line in Fig. 7) [35,36].

One of the primary objectives of using ATR-FTIR was to confirm the presence of the HEMA-co-PFDA copolymer, on the membrane surface after the fouling. This was accomplished by the presence of the peaks at ~1,240 and ~1,205 cm^{-1}in the zoomed FTIR spectra in spectral range of 1,160–1,260 cm^{-1} (Fig. 8). These peaks can be associated to the symmetric and asymmetric stretching of the pendant fluoroalkyl chain present in the PFDA molecule [16,37] and confirms the presence of the HEMA-PFDA copolymer film on membrane surface.

Stronger FTIR peaks at ~1,240 and ~1,205 cm^{-1}in the modified Koch membranes (Fig. 8(a) and (b)) confirm the presence of the HEMA-PFDA copolymer film after 6 h of fouling runs in the presence of SA even at higher pressure (800 psi). From Fig. 8, it is also clear

that this peak is more pronounced in the modified membranes as compared to the unmodified membranes, which indicates that the deposited HEMA-PFDA copolymer film is rather stable under alginate exposure for the entire duration (6 h) at higher pressure (800 psi).

4. Conclusions

iCVD is a facile method that can be used to modify surface of delicate substrate, such as RO membranes, for enhancing biofouling and organic fouling with minimal effects on membranes performance. The surface-modified Koch membranes with an ultrathin layer (~35 nm) of HEMA-co-40% PFDA copolymer films resulted in much lower flux decline with nearly unaffected salt rejection performance when compared to the bare Koch membranes. Structure of the deposited foulant (SA) layer on the surfaces of the modified Koch membranes was sporadic and porous as opposed to more continuous and dense foulant deposition onto unmodified Koch membranes. This marked difference in the structure of deposited foulant is strong evidence that HEMA-PFDA copolymer film discourages foulant attachment onto the membrane surface. The porous structure of the foulant is also reflected in a much lower permeate flux decline observed only for the modified Koch membranes

under cross-flow filtration tests. ATR-FTIR results suggest that the HEMA-co-40% PFDA film remains stable even after 6 h of exposure to SA at operating pressure as high as 800 psi. Encouraged by these preliminary findings, future work is planned to investigate and evaluate the organic fouling resistance of the surface-modified RO membranes under higher salt loadings and under aggravated foulant conditions.

Acknowledgment

References

[1] A. Matin, Z. Khan, S. Zaidi, M. Boyce, Biofouling in reverse osmosis membranes for seawater desalination: Phenomena and prevention, Desalination 281 (2011) 1–16.

[2] A. Matin, G. Ozaydin-Ince, Z. Khan, S.M.J. Zaidi, K. Gleason, D. Eggenspiler, Random copolymer films as potential antifouling coatings for reverse osmosis membranes, Desalin. Water Treat. 34 (2011) 100–105.

[3] H.Z. Shafi, Z. Khan, R. Yang, K.K. Gleason, Surface modification of reverse osmosis membranes with zwitterionic coating for improved resistance to fouling, Desalination 362 (2015) 93–103.

[4] S.-H.Cho., P.V.X. Hung, J.-J. Woo, S.-H. Moon, Behaviors of commercialized seawater reverse osmosis membranes under harsh organic fouling conditions, Desalin. Water Treat. 15 (2010) 48–53.

[5] B. Kwon, H.K. Shon, J. Cho, Investigating the relationship between model organic compounds and ultrafiltration membrane fouling, Desalin. Water Treat. 8 (2009) 177–187.

[6] C. Jarusutthirak, G. Amy, J.-P. Croué, Fouling characteristics of wastewater effluent organic matter (EfOM) isolates on NF and UF membranes, Desalination 145 (2002) 247–255.

[7] M. Into, A.-S. Jönsson, G. Lengdén, Reuse of industrial wastewater following treatment with reverse osmosis, J. Membr. Sci. 242 (2004) 21–25.

[8] Q. Li, M. Elimelech, Organic fouling and chemical cleaning of nanofiltration membranes: Measurements and mechanisms, Environ. Sci. Technol. 38 (2004) 4683–4693.

[9] S. Hong, M. Elimelech, Chemical and physical aspects of natural organic matter (NOM) fouling of nanofiltration membranes, J. Membr. Sci. 132 (1997) 159–181.

[10] Q. Li, Z. Xu, I. Pinnau, Fouling of reverse osmosis membranes by biopolymers in wastewater secondary effluent: Role of membrane surface properties and initial permeate flux, J. Membr. Sci. 290 (2007) 173–181.

[11] A. Asatekin, A. Menniti, S. Kang, M. Elimelech, E. Morgenroth, A.M. Mayes, Antifouling nanofiltration membranes for membrane bioreactors from self-assembling graft copolymers, J. Membr. Sci. 285 (2006) 81–89.

[12] A. Matin, Z. Khan, K. Gleason, M. Khaled, S. Zaidi, A. Khalil, P. Moni, R. Yang, Surface-modified reverse osmosis membranes applying a copolymer film to reduce adhesion of bacteria as a strategy for biofouling control, Sep. Purif. Technol. 124 (2014) 117–123.

[13] G. Ozaydin-Ince, A. Matin, Z. Khan, S. Zaidi, K.K. Gleason, Surface modification of reverse osmosis desalination membranes by thin-film coatings deposited by initiated chemical vapor deposition, Thin Solid Films 539 (2013) 181–187.

[14] G. Ozaydin-Ince, K.K. Gleason, Transition between kinetic and mass transfer regimes in the initiated chemical vapor deposition from ethylene glycol diacrylate, J. Vac. Sci. Technol. A 27 (2009) 1135–1143.

[15] S.H. Baxamusa, S.G. Im, K.K. Gleason, Initiated and oxidative chemical vapor deposition: A scalable method for conformal and functional polymer films on real substrates, Phys. Chem. Chem. Phys. 11 (2009) 5227–5240.

[16] A. Matin, H.Z. Shafi, Z. Khan, M. Khaled, R. Yang, K. Gleason, F. Rehman, Surface modification of seawater desalination reverse osmosis membranes: Characterization studies & performance evaluation, Desalination 343 (2014) 128–139.

[17] A. Matin, H. Shafi, Z. Khan, M. Khaled, R. Yang, K. Gleason, F. Rehman, Surface modification of seawater desalination reverse osmosis membranes: Characterization studies & performance evaluation, Desalination 343 (2014) 128–139.

[18] G. Ozaydin-Ince, A. Matin, Z. Khan, S.J. Zaidi, K.K. Gleason, Surface modification of reverse osmosis desalination membranes by thin-film coatings deposited by initiated chemical vapor deposition, Thin Solid Films 539 (2013) 181–187.

[19] S.H. Baxamusa, K.K. Gleason, Random copolymer films with molecular-scale compositional heterogeneities that interfere with protein adsorption, Adv. Funct. Mater. 19 (2009) 3489–3496.

[20] A.K. Ghosh, E.M. Hoek, Impacts of support membrane structure and chemistry on polyamide–polysulfone interfacial composite membranes, J. Membr. Sci. 336 (2009) 140–148.

[21] E.-S. Kim, Y.J. Kim, Q. Yu, B. Deng, Preparation and characterization of polyamide thin-film composite (TFC) membranes on plasma-modified polyvinylidene fluoride (PVDF), J. Membr. Sci. 344 (2009) 71–81.

[22] H.I. Kim, S.S. Kim, Plasma treatment of polypropylene and polysulfone supports for thin film composite reverse osmosis membrane, J. Membr. Sci. 286 (2006) 193–201.

[23] A. Matin, H. Shafi, M. Wang, Z. Khan, K. Gleason, F. Rahman, Reverse osmosis membranes surface-modified using an initiated chemical vapor deposition technique show resistance to alginate fouling under cross-flow conditions: Filtration & subsequent characterization, Desalination 379 (2016) 108–117.

[24] A. Widjaya, T. Hoang, G.W. Stevens, S.E. Kentish, A comparison of commercial reverse osmosis membrane characteristics and performance under alginate fouling conditions, Sep. Purif. Technol. 89 (2012) 270–281.

[25] G.M. Geise, H.S. Lee, D.J. Miller, B.D. Freeman, J.E. McGrath, D.R. Paul, Water purification by membranes: The role of polymer science, J. Polym. Sci. Part B Polym. Phys. 48 (2010) 1685–1718.

[26] B. Kwon, S. Lee, J. Cho, H. Ahn, D. Lee, H.S. Shin, Biodegradability, DBP formation, and membrane fouling potential of natural organic matter: Characterization and controllability, Environ. Sci. Technol. 39 (2005) 732–739.

[27] A. Matin, Z. Khan, K. Gleason, M. Khaled, S. Zaidi, A. Khalil, P. Moni, R. Yang, Surface-modified reverse osmosis membranes applying a copolymer film to reduce adhesion of bacteria as a strategy for biofouling control, Sep. Purif. Technol. 124 (2014) 117–123.

[28] J. Wu, A.E. Contreras, Q. Li, Studying the impact of RO membrane surface functional groups on alginate fouling in seawater desalination, J. Membr. Sci. 458 (2014) 120–127.

[29] A.E. Contreras, Z. Steiner, J. Miao, R. Kasher, Q. Li, Studying the role of common membrane surface functionalities on adsorption and cleaning of organic foulants using QCM-D, Environ. Sci. Technol. 45 (2011) 6309–6315.

[30] Q. An, F. Li, Y. Ji, H. Chen, Influence of polyvinyl alcohol on the surface morphology, separation and anti-fouling performance of the composite polyamide nanofiltration membranes, J. Membr. Sci. 367 (2011) 158–165.

[31] C.Y. Tang, Y.-N. Kwon, J.O. Leckie, Characterization of humic acid fouled reverse osmosis and nanofiltration membranes by transmission electron microscopy and streaming potential measurements, Environ. Sci. Technol. 41 (2007) 942–949.

[32] S. Lee, M. Elimelech, Relating organic fouling of reverse osmosis membranes to intermolecular adhesion forces, Environ. Sci. Technol. 40 (2006) 980–987.

[33] C.Y. Tang, Y.-N. Kwon, J.O. Leckie, Probing the nano—And micro-scales of reverse osmosis membranes—A comprehensive characterization of physiochemical properties of uncoated and coated membranes by XPS, TEM, ATR-FTIR, and streaming potential measurements, J. Membr. Sci. 287 (2007) 146–156.

[34] C.Y. Tang, Y.-N. Kwon, J.O. Leckie, Effect of membrane chemistry and coating layer on physiochemical properties of thin film composite polyamide RO and NF membranes: I FTIR and XPS characterization of polyamide and coating layer chemistry, Desalination 242 (2009) 149–167.

[35] M.K. Trivedi, Characterization of physicochemical and thermal properties of chitosan and sodium alginate after biofield treatment, Pharm. Anal. Acta 6(10) (2015) 1–9, doi: 10.4172/21532435.1000430.

[36] R. Mishra, K. Ramasamy, S. Lim, M. Ismail, A. Majeed, Antimicrobial and *in vitro* wound healing properties of novel clay based bionanocomposite films, J. Mater. Sci. Mater. Med. 25 (2014) 1925–1939.

[37] D. Lin-Vien, N.B. Colthup, W.G. Fateley, J.G. Grasselli, The Handbook of Infrared and Raman Characteristic Frequencies of Organic Molecules, Elsevier, San Diego, California, 1991.